Atomistic modeling of the polarization of nitrogen centers in diamond due to growth surface orientation

M. K. Atumi,* J. P. Goss, and P. R. Briddon
School of Electrical and Electronic Engineering, Newcastle University, Newcastle upon Tyne NE1 7RU, United Kingdom

M. J. Rayson
Department of Chemistry, University of Surrey, Guildford, Surrey GU2 7XH, United Kingdom
(Received 17 September 2013; revised manuscript received 8 November 2013; published 3 December 2013)

Diamond, as a consequence of its superlative intrinsic physical properties, is an attractive material for a wide range of applications. Recent developments have greatly enhanced the quality of gas-phase grown diamonds. It has been observed that some defects are grown into diamond preferentially aligned to specific orientations with respect to growth surface. Of particular note, the nitrogen-vacancy center is polarized in (110)-grown material. Preferential alignment of these defects in diamond may enhance their use in applications such as quantum information and encryption, and in diamond-based magnetometers. The origin of the preferential orientation with respect to the growth surface is not completely understood, and a mechanistic model is highly desirable in order that one might both optimize defect incorporation and better understand the growth of diamond in a wider sense. We present the results of quantum-chemical simulations that provide insight into the preferential alignment of nitrogen-related defects grown into different diamond surface orientations, showing that the sequence of structure surfaces required to produce polarization aligns with their energies.

DOI: 10.1103/PhysRevB.88.245301 PACS number(s): 81.05.ug, 61.72.jn, 61.72.Bb, 81.10.Aj

I. INTRODUCTION

Diamond, the hardest known naturally occurring material, has a wide band gap, high thermal conductivity,[1] large breakdown field,[2] high intrinsic carrier mobility,[3] and optical transparency in the infrared region, making it an interesting material for many applications. Although boron is present in relatively rare natural diamonds, it is readily incorporated in synthetic material, where it can produce *p*-type, metallic,[4,5] and even superconducting samples.[6,7] More commonly seen in natural diamond than boron, and also easily incorporated in synthetic material, is nitrogen. Indeed, the incorporation of nitrogen has a large effect on the structural and morphological properties of chemical vapor deposition (CVD) diamond, and relatively low concentrations of nitrogen in the gas phase can significantly affect growth rates.[8–10]

In as-grown CVD diamond, the most common form adopted by nitrogen is the single substitutional center (N_s), which is labeled the P1 center when observed in electron paramagnetic resonance (EPR), and the C center as seen in infrared absorption. N_s is a deep donor, with an ionization energy[11] of around 1.7 eV, too large to be usefully electrically active at room temperature. The deep donor behavior may be traced to a structural rearrangement,[12–17] so that one of the four N–C bonds is extended by 30–40 %, forming a C_{3v} symmetry center with two states in the band gap: the N lone-pair state lies a little above the valence band, and in the upper half of the band gap a state associated with the carbon radical formed by the extension of the N–C bond is half-filled. In the positive charge state, nitrogen is isoelectronic with carbon, and N_s adopts an on-site, tetrahedral geometry. N_s may also act as an acceptor,[18,19] with the electron being localized at the unique carbon site, resulting in a lone pair on the carbon and an even greater degree of dilation.

Another frequently observed form of nitrogen in as-grown CVD diamond is the nitrogen-vacancy (NV) center, either by growing in as a unit or by N_s trapping mobile vacancies. NV may also be formed by post-growth irradiation and heat treatment of diamond containing N_s: irradiation creates vacancies in the diamond, which become mobile at ~800 K, which then become trapped adjacent to the immobile nitrogen impurities,[20,21] with a theoretical[22] binding energy of 3.3 eV. In the neutral charge state, NV is identified[23] by a zero-phonon line at 2.156 eV, but the arguably more interesting negative charge state emits[24] at 1.945 eV. Previous density functional theory (DFT) calculations using a very similar methodology to that employed in the current study predict[25] donor and acceptor levels for NV at $E_v + 1.5$ eV and $E_c - 3.3$ eV, respectively. More recent studies employing more advanced computational techniques also place a donor level a little above the valence-band top and a midgap acceptor level,[26,27] lending support to the approach we have adopted. Experimentally, the acceptor state lies at 2.58 eV from a band edge, as estimated from a photoionization threshold around 480 nm.[28] The negatively charged center has a spin-triplet ground state, which has recently been exploited for quantum-state-based applications including quantum computing and encryption,[29,30] magnetometry,[31–36] and magnetic-field-based sensing.[37]

In addition to the formation of NV centers in CVD grown diamond, a complex of NV with a single hydrogen atom has also been identified.[38–40] It is not seen in natural diamond, and is thought to exist in the negative or neutral charge states.[39–42] The NVH center is seen in EPR as an $S = 1/2$ defect (the negative charge state), but with C_{3v} symmetry, which can be explained by the rapid reorientation of the hydrogen between the three carbon radicals.[39,43,44]

In addition to the composition of these important defects in CVD diamond, both vacancy-containing centers are grown into diamond with a nonrandom population of the various symmetrically equivalent orientations.[45] In (110)-oriented substrates, the centers are preferentially aligned in two of four

⟨111⟩ directions with equal probability, and they do not appear in the other orientations at all.

Typically, diamond CVD takes place in the 700–1000 °C range, with the samples used in the experimental identification of polarization being in line with this practice.[45] Importantly, there is a wealth of observation regarding the migration of N_s and N*V* centers, with temperatures far above those used in CVD being required. For example, the process by which N_s aggregates into pairs is activated by around[46] 5 eV, and N*V* centers typically begin to migrate at high temperatures, annealing out above[47] around 1500 °C. It is generally believed that N*V* centers migrate via a mechanism which involves its reorientation, so that both reorientation and migration are insignificant in as-grown CVD diamond. N*V*H is also thermally stable,[40] annealing out well above growth temperatures, being in excess of 2000 K. In contrast, as mentioned above, monovacancies migrate even at low growth temperatures. In light of the relative mobility of monovacancies, and the immobility of N_s, N*V*, and N*V*H, the model for the incorporation of these centers takes on more significance in light of the polarization: it is implausible that a migrating vacancy would always result in the same polarization, so N*V* and N*V*H centers must grow in as units. The proposal[45] is then that the N atom is fully chemically bonded into the surface first, and that the subsequent layer of diamond grown over the (110) layer containing the nitrogen occasionally leaves a vacant site above it.

Although the mechanism seems plausible, it requires direct quantitative analysis, which is extremely challenging to obtain directly from the experiment. In contrast, atomistic, quantum-chemical modeling can provide immediate insight into the processes, allowing for the proposed mechanism to be evaluated. A detailed understanding of the processes involved may in turn provide a route to optimization of the incorporation or exclusion of such point defects, and furthermore provide further insight into the processes underpinning diamond growth and perhaps ultimately clarify the role of impurity incorporation within surface morphology and diamond growth rate.

Therefore, we have performed a density functional theory analysis of N_s, N*V*, and N*V*H centers in diamond, and we investigate the polarization of these defects with respect to not only the (110) H-terminated surface for which polarization of these centers has been observed, but also (111) and (001) surfaces to place the (110) surface energetics in context. We first outline the methodology.

II. METHOD

All results presented in this paper are based upon density functional simulations. Calculations were carried out using the generalized-gradient approximation (GGA),[48] as implemented[49,50] in the AIMPRO (Ab Initio Modeling PROgram). The Kohn-Sham functions are expanded using a Gaussian basis set,[51] and matrix elements of the Hamiltonian are determined using a plane-wave expansion of the density and Kohn-Sham potential[52] with a cutoff of 175 Ha. The Gaussian functions are atom-centered, and for each C atom they are constituted from eight fixed linear combinations of *s* and *p* orbitals, plus a set of *d* functions for polarizations.

TABLE I. Surface lattice vectors in units of a_0, composition, and number of atomic layers of carbon (n) in the slab supercells used in this study.

Orientation	$\vec{v}_1$	$\vec{v}_2$	Composition	n
(110)	$3[110]/\sqrt{2}$	2[001]	$C_{144}H_{24}$	12
(110)	$4[110]/\sqrt{2}$	3[001]	$C_{288}H_{48}$	12
(111)	$3[1\bar{1}0]/\sqrt{2}$	$3[10\bar{1}]/\sqrt{2}$	$C_{126}H_{18}$	14
(001)	$4[110]/\sqrt{2}$	$3[1\bar{1}0]/\sqrt{2}$	$C_{192}H_{24}$	16

This constitutes a basis of 13 functions per C atom. The N atoms are represented by basis sets made up from independent sets of *s*, *p*, and *d* functions with four widths (constituting 40 functions per atom) and H by three widths of *s* and *p* functions (16 functions per atom). A similar approach was previously used successfully to study the electronic structure of different diamond surfaces.[53–55]

For bulk diamond, our approach yields a lattice constant and bulk modulus of 3.573 Å and 440 GPa, in good agreement with experiment. It is known that the GGA functional adopted for this study leads to an underestimate in the band gap relative to experiment, which has an impact upon the interpretation of quantities such as optical and electrical transitions at a quantitative level. However, we note that previous publications in which AIMPRO has been employed using generalized-gradient and local-density approximations and otherwise very similar approximations as used here have been shown to be quantitatively accurate in comparison with experiment, e.g., in defect-complex binding energies,[56] hyperfine interactions at N-containing centers in diamond, which depend critically upon the accuracy of the spin density,[17] and diamond-surface properties such as electron affinities.[53,54] Although alternative approaches such as hybrid functionals, screened exchange, or self-interaction corrections may result in slightly different values for relative energies, and in particular provide a potentially more reliable estimate of the location of gap levels, based upon the agreement with experiment in relevant comparative cases, we expect the current methodology to be sufficient to be conclusive.

Diamond surfaces have been simulated using the standard slab-geometry approach, with the base unit cells as detailed in Table I. To study N_s, N*V*, and N*V*H centers in the three diamond surfaces, the nitrogen atom was placed in each of the upper six, seven, and eight layers of the (110), (111), and (001) diamond slabs, respectively, as illustrated in Fig. 1. In each case there are multiple defect orientations relative to the surface normal, all of which have been included in the analysis. For example, for N_s in the (110) surface, there are three distinct orientations: [111], $[\bar{1}\bar{1}1]$, and either $[\bar{1}1\bar{1}]$ or $[1\bar{1}\bar{1}]$ directions, which are equivalent. A vacuum layer of ∼0.6 nm was used in all cases, sufficient for the electrostatic potential to reach the vacuum limit. In all cells, both surfaces were terminated by hydrogen.

For a reference calculation, the P1 center was simulated in a 216-atom supercell ($C_{215}N_1$) made up from $3 \times 3 \times 3$ conventional, eight-atom unit cells.

The Brillouin zone was sampled using the Monkhorst-Pack scheme.[57] For surfaces, since there is no dispersion in the

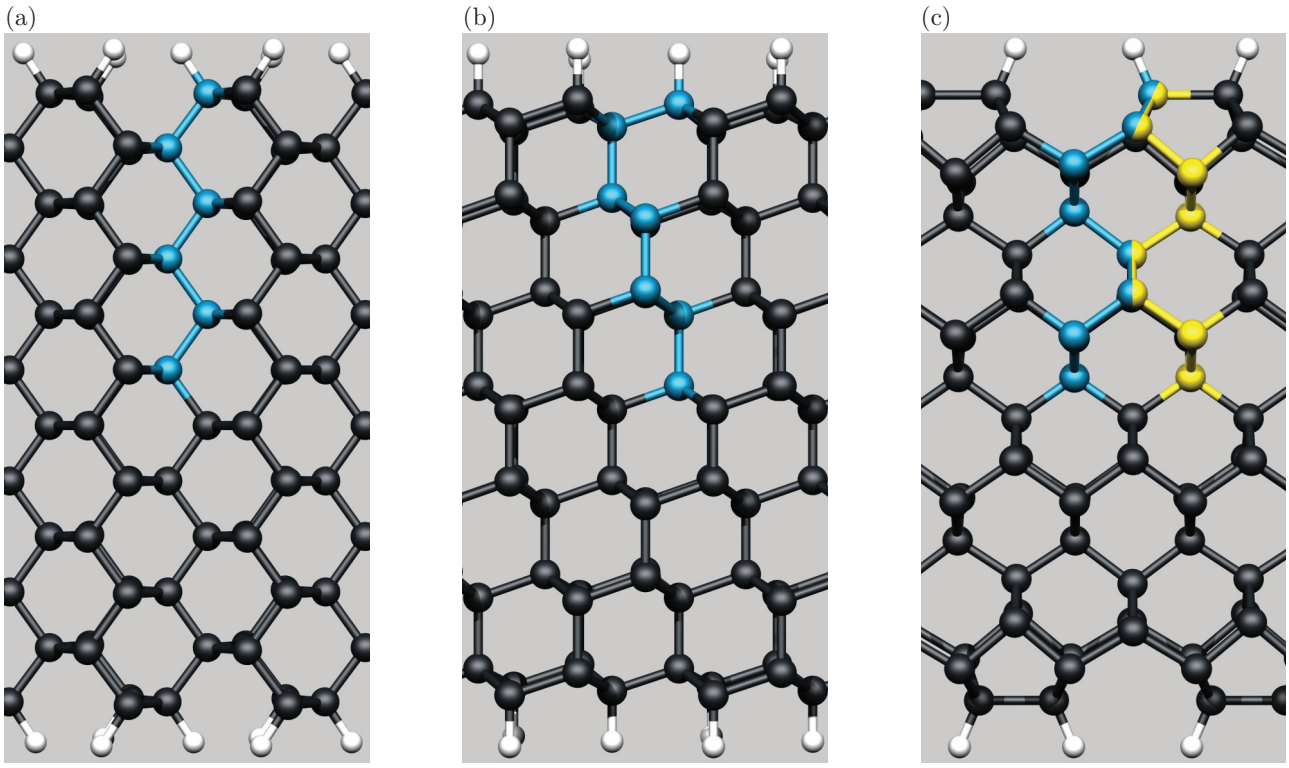

FIG. 1. (Color online) Schematics of the H-terminated (a) (110), (b) (111), and (c) (001) diamond surfaces slabs. Black and white spheres indicate C and H, respectively, with the blue sites indicating the range of sites in which N has been substituted. For the (001) surface, the yellow spheres indicate the alternative line of sites in the slab, as described in the text. For the three slabs, the surface normals are vertically up, with the projections being in the (a) $[1\bar{1}0]$, (b) $[\bar{1}10]$, and (c) $[1\bar{1}0]$ direction, and the horizontal directions being (a) [001], (b) $[11\bar{2}]$, and (c) [110], respectively.

surface normal direction, the Brillouin zone is effectively two-dimensional, and for the (110), (111), and (001) surfaces, 3×3, 3×3, and 4×3 meshes were used, respectively. The convergence of the total energy with respect to the sampling was established at less than 5 meV. For the reference P1 center, a $2 \times 2 \times 2$ sampling scheme was used.

Optimization of the structures is performed using a conjugate gradients scheme. In determination of the equilibrium structures, all atoms were allowed to move. The impact of whether the bottom surfaces of the slabs were fixed or relaxed during optimization was assessed, and total energies were found to be independent of this choice to within around 60 meV. For activation energies, the climbing nudged elastic band (NEB) method has been used.[58,59]

To allow for a comparison between different surface orientations, and between defects comprised of different numbers of atoms, it is necessary to evaluate formation energies, which may be calculated for a system X using

$$E^f(X) = E^{\text{tot}}(X) - \sum \mu_j, \tag{1}$$

where $E^f(X)$ is the formation energy, $E^{\text{tot}}(X)$ is the total energy, and μ_j are the chemical potentials of the atomic species, respectively. Since we are primarily interested in the energy differences of the point defects in different locations, it is important that we exclude contributions to the formation energy due to the different surfaces, so an alternative approach has been adopted. The formation energy of the defect alone may be obtained,

$$E^f(X) = E^{\text{tot}}(X) - E^{\text{tot}}(\text{slab}) - \sum \mu_j, \tag{2}$$

where $E^{\text{tot}}(\text{slab})$ is the total energy of the defect-free slab. The chemical potentials are then defined as follows. The carbon chemical potential, μ_{C}, is the energy per atom of bulk diamond. The hydrogen chemical potential is taken to be the average energy per hydrogen atom for the three low-index surfaces explored in this study, where for the slab cell C_nH_m, the average energy is calculated as $[E^{\text{tot}}(\text{slab}) - n\mu_{\text{C}}]/m$. The nitrogen chemical potential is obtained from the condition of zero formation energy for N_s in a 216-atom bulk diamond simulation. Although this condition may be viewed as somewhat arbitrary, since all N-containing centers examined in this study contain only single N atoms, the choice of μ_{N} only defines the zero of the formation energy scale, and it has no impact on formation energy differences. In addition, this condition gives a convenient immediate comparison for the energies relative to a relatively common defect center.

Finally, for electrical levels, it would also be necessary to take into account the impact of the Fermi energy, and to include energies of charged defects. Formation energies for charged supercells include terms[60] of the form $q[E_v(X,q) + \mu_e]$ and $\chi(X,q)$, where q is the charge state, $E_v(X,q)$ is the energy of the valence-band top for the system X, and $\chi(X,q)$ represents a correction for periodic boundary conditions, typically including terms in charge and multipole interactions.

However, in this study, we are only interested in the *relative* locations of the levels at various sites with respect to the surface, and under the approximation that the additional terms in the formation energies are largely systematic, we only present donor and acceptor level *differences* in this paper, where the contributions from the periodic boundary condition error, and the location of the Fermi energy, play no role.

III. RESULTS

N_s, NV, and NVH centers have been modeled on and below (110), (111), and (001) diamond surfaces as a function of depth, with the N components of the defects as shown schematically in Fig. 1. As mentioned in Sec. II, the defects were modeled in all orientations, and we present the results of the simulations organized in the following way. We first present the results for the simple substitutional nitrogen center for each surface orientation, including the impact of the proximity of the surface upon the structure, orientational anisotropy, energetics, and electrical levels. We then repeat a similar analysis for NV and NVH centers before making a comparison between the three forms of N-containing defects, including the energetic basis for the existence of polarization in (110)-grown samples.

A. N_s centers

Figure 2 shows the formation energies as a function of depth, including the various orientations of the broken bond.

Figure 2(a) represents the data for the (110) surface. When N_s is in the uppermost carbon layer, there are essentially three possibilities. A bond may be broken in line with the P1-EPR center in two ways, either a bond within the plane of the surface (i.e., either $[1\bar{1}1]$ or $[\bar{1}11]$) or one *into* the surface along $[\bar{1}\bar{1}\bar{1}]$. The relative formation energy between these two cases is independent of the atomic chemical potentials, and the latter form is found to be energetically favored by around 0.5 eV.

The third option involves the removal of the H atom along [111] (the natural consequence of a "broken bond" out of the surface), resulting in a completely chemically satisfied system. This differs from the other two forms in composition (there is one fewer H atom), and the relative formation energy thus depends upon μ_{H}. Using the chemical potentials defined in Sec. II, E^f for N_s at the surface with a H atom removed is -3.2 eV, some 2.6 eV below that of the P1-like structure polarized into the surface. Despite it being significantly more stable at the surface, removal of a surface H atom is much less favorable when the N is buried deep within the diamond. Such structures can be viewed as a carbon radical at the surface accepting an electron from the N donor, forming a lone pair at the surface and an ionized P1 center in the diamond. The energy of such an arrangement rapidly increases, and is only of any significance for N in the first three atomic layers of carbon.

For the P1-like structures, polarization within the (110) plane is generally less favorable than the alternatives, a consequence of the relative ease with which strain is accommodated by displacement normal to the surface. Figure 2 shows that beyond the third layer (i.e., beyond just ∼3 Å), the formation energies of the P1-like structures converge to zero to within

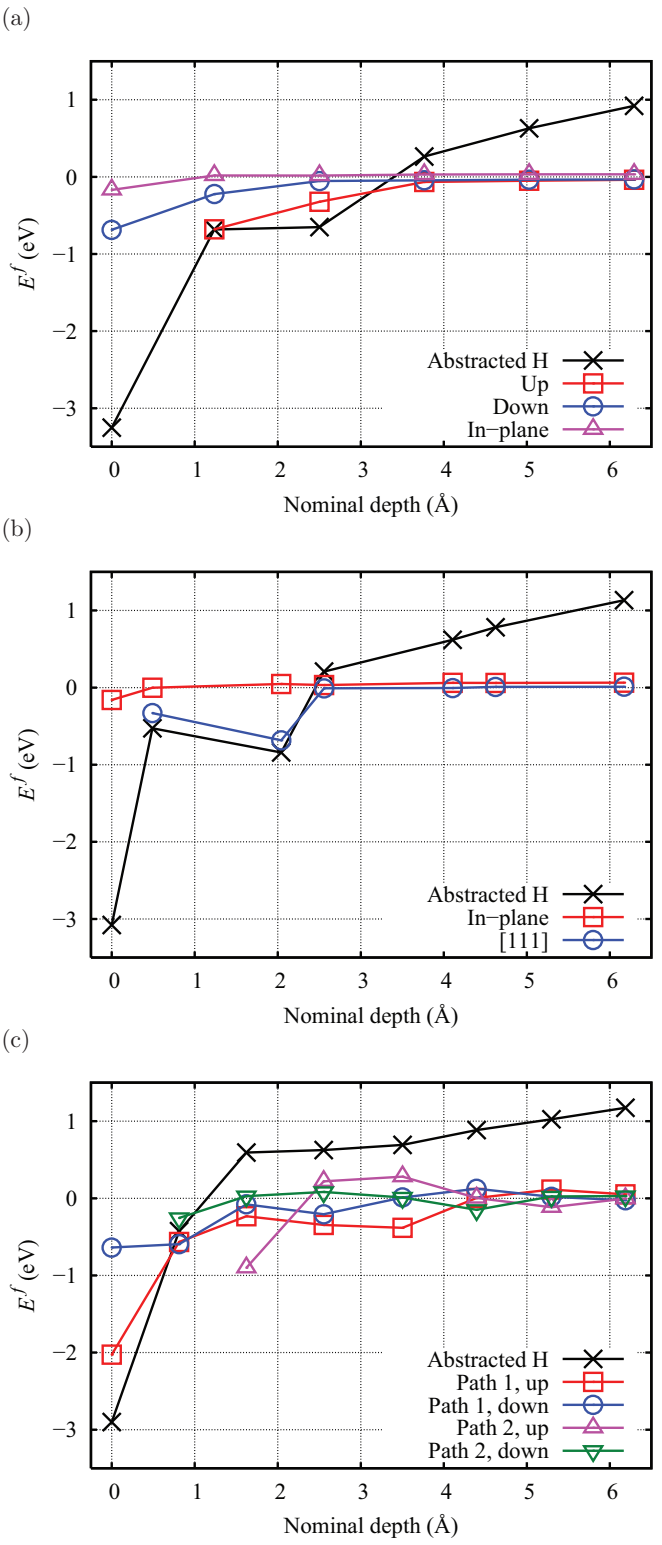

FIG. 2. (Color online) Formation energy of N_s in (a) (110), (b) (111), and (c) (001) diamond surfaces as a function of depth of the carbon site in pristine diamond (Fig. 1), as specified by Eq. (2). In each case, "up" and "down" refer to the polarization of the dilated N–C bond relative to the N atom, with respect to the surface plane. For the (111) system, the circles represent polarization parallel to the surface normal, and for the (001) surface, the two paths are as shown in Fig. 1. "Abstracted H" refers to structures where a hydrogen atom has been removed from a surface site above the nitrogen.

a few 10s of meV. The approach to zero is a consequence of the definition of μ_N, with the small variations ascribed to anisotropy in the supercell approximation. We have calculated sample structures in a supercell with the larger surface area (Table I), and for P1-like structures in the core of the slab the formation energies differ from zero by just 30 meV.

The variation in energy in the first few layers is also associated with changes in geometry. The length of the broken bond, plotted in Fig. 3(a), increases with decreasing energy; in cases such as N in the second layer and the radial in the first layer where the energy is relatively low, this effect is clear, with the N–C distance being 30% greater than the value in bulk diamond.

The final aspect we review is the variation in electrical behavior with depth. To determine the donor and acceptor levels, positively and negatively charged N_s have also been optimized for each position. A determination of the location of the levels within the band gap is not the focus of this study, but rather the change in the location as a function of depth. We have therefore calculated differences in the ionization energies and electron affinities relative to those at the deepest sites available in the simulations. The results for the (110) surface are plotted in Fig. 4(a). Where N_s is four or more layers into the diamond, the donor and acceptor levels are constant to within computational uncertainties. The splitting in the levels for different orientations arises from the finite in-plane interactions between the periodic images. However, they are much smaller than the variation in the electrical levels as a function of depth, and they do not affect our conclusions.

There are some interesting effects resolved in the electrical levels in the close surface region. First, the donor level is significantly deeper (further from the conduction-band minimum), which reflects the extra dilation of the unique N–C direction [Fig. 3(a)] afforded by the relatively less constrained surface. It is also possible to see by comparing with Fig. 2(a) that the deeper levels correspond to the more stable orientations and depths, as one might expect.

We now turn to the (111) surface, for which the energetics are illustrated in Fig. 2(b). As with the (110) surface, the scope for relaxation at the surface is reflected in the energies: N_s at the surface with a H atom removed is by far the most energetically favorable structure. This structure is shown in Fig. 5(b). In addition, for N_s in the *third* layer and the broken bond along [111], the unique carbon site is able to relax significantly [Figs. 3(b) and 5(d)], becoming approximately coplanar with the three carbon neighbors in the uppermost layer. Such structures are 0.7 eV lower in energy than P1 centers located in bulk diamond. The intermediate, second-layer site is relatively less stable due to the constrained environment for the carbon radical site [Fig. 5(c)].

Finally, we turn to the (001) surface, with the energetics presented in Fig. 2(c). They follow the pattern of the other two surface orientations, with N in a surface site being energetically most favorable. Another relatively low-energy structure with N in the surface layer may be generated by retaining the H atom but breaking the reconstruction along [110]. The resulting N–C separation is approximately the host second-neighbor distance [Fig. 3(c)]. The formation energy is just 0.9 eV higher than the chemically satisfied system with a hydrogen atom removed.

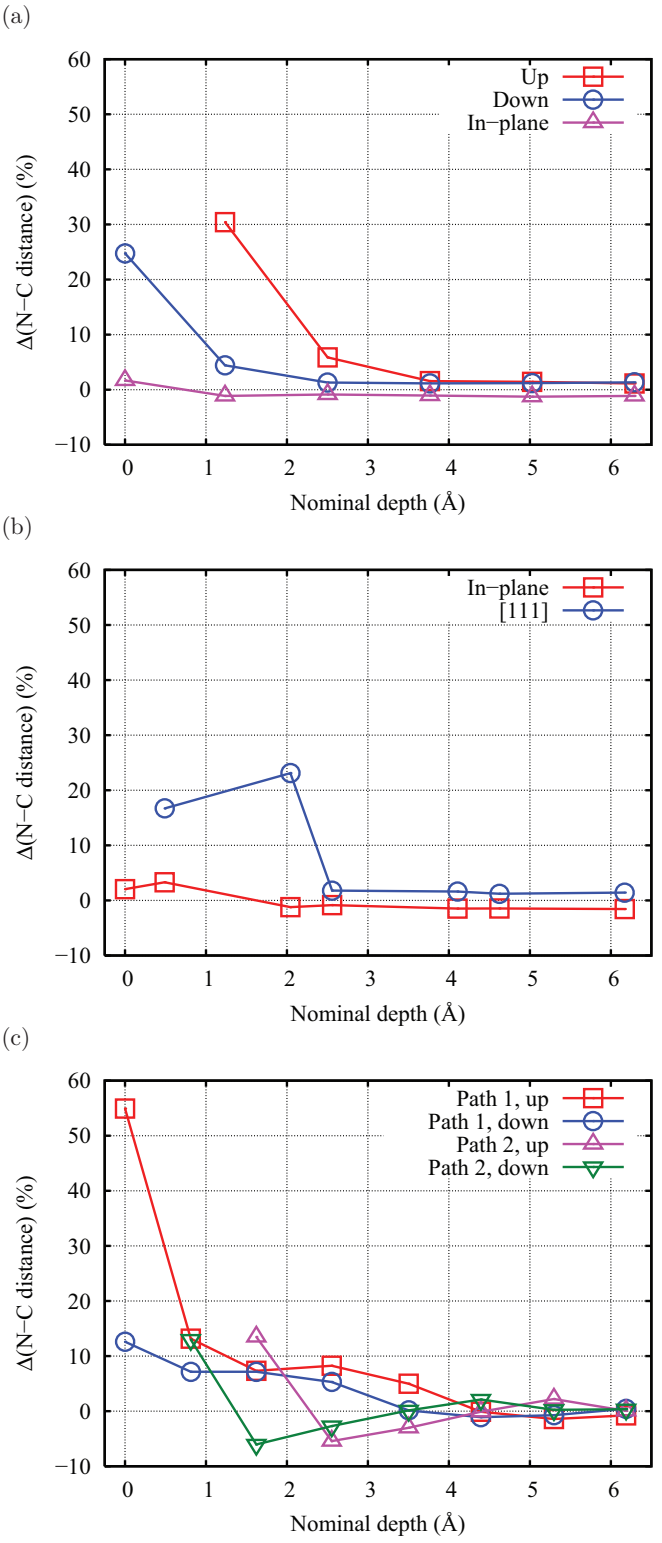

FIG. 3. (Color online) Fractional difference in the distance between the nitrogen and radical carbon atoms relative to the value calculated for P1 in bulk diamond for (a) (110), (b) (111), and (c) (001) diamond surfaces and as a function depth. Symbols follow the definition in Fig. 2.

Unlike the (110) and (111) surfaces, there is more than one site in each atomic layer (it may be either under a reconstruction or a trough), so that there are many more nonequivalent

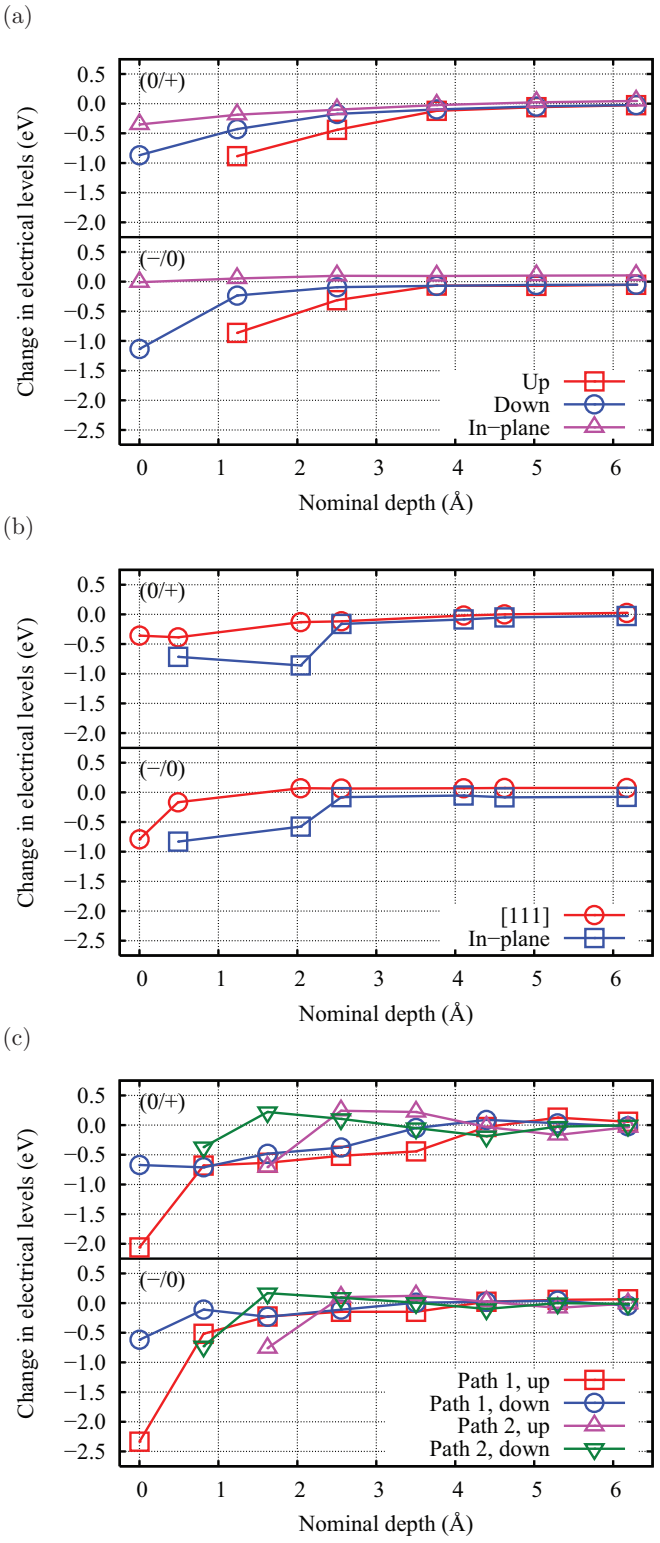

FIG. 4. (Color online) Calculated changes in donor [labeled (0/+)] and acceptor [labeled (−/0)] levels for N_s in (a) (110), (b) (111), and (c) (001) diamond surfaces and as a function depth. A positive change indicates that the level is moving upward in energy, away from the valence-band top. Symbols follow the definition of Fig. 2.

sites and orientations to consider in the (001) case. In the third, fourth, seventh, and eighth layers, there are two distinct

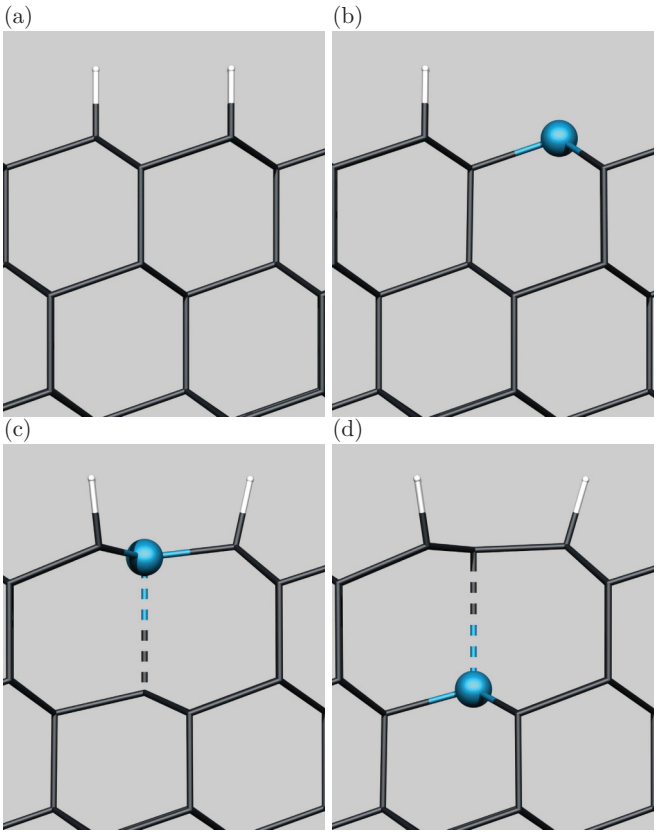

FIG. 5. (Color online) Schematics of the structures of N_s in the (111) surface. Parts (b)–(d) show the lowest-energy forms for the first to third layers, respectively, with (a) being the corresponding defect-free section, for comparison. Colors are as in Fig. 1. [111] is vertically up, with the projection and horizontal direction being $[\bar{1}10]$ and $[11\bar{2}]$, respectively.

sites, but in each case there are only two orientations (either polarized with a component toward the surface, or away from it), whereas in the first, second, fifth, and sixth layers there is only one site, but three orientations are nonequivalent. Thus there are either three or four configurations at each depth, all of which have been considered. Below around 4 Å, the effect of the surface is no longer resolved in the calculations.

It is helpful at this stage to make some general observations across all three surfaces. Despite the variation in the details of the properties of N_s in the different surfaces, there are many similarities, and the impact of the surface is lost beyond 3–4 Å. The most favorable location of nitrogen is at the very surface, with N_s substituting for a C–H group. Such arrangements as calculated using the chemical potentials for the atomic species as defined in Sec. II are 2.9–3.2 eV lower in energy than a fully hydrogenated surface with a neutral P1 center buried deep within the diamond slab.

B. NV centers

We now turn to the case in which N_s captures a lattice vacancy. As with N_s, NV contains a threefold-coordinated nitrogen atom with a lone pair pointed toward the center of the defect, but NV contains three rather than a single carbon radical, resulting in a degenerate state around midgap. This in turn

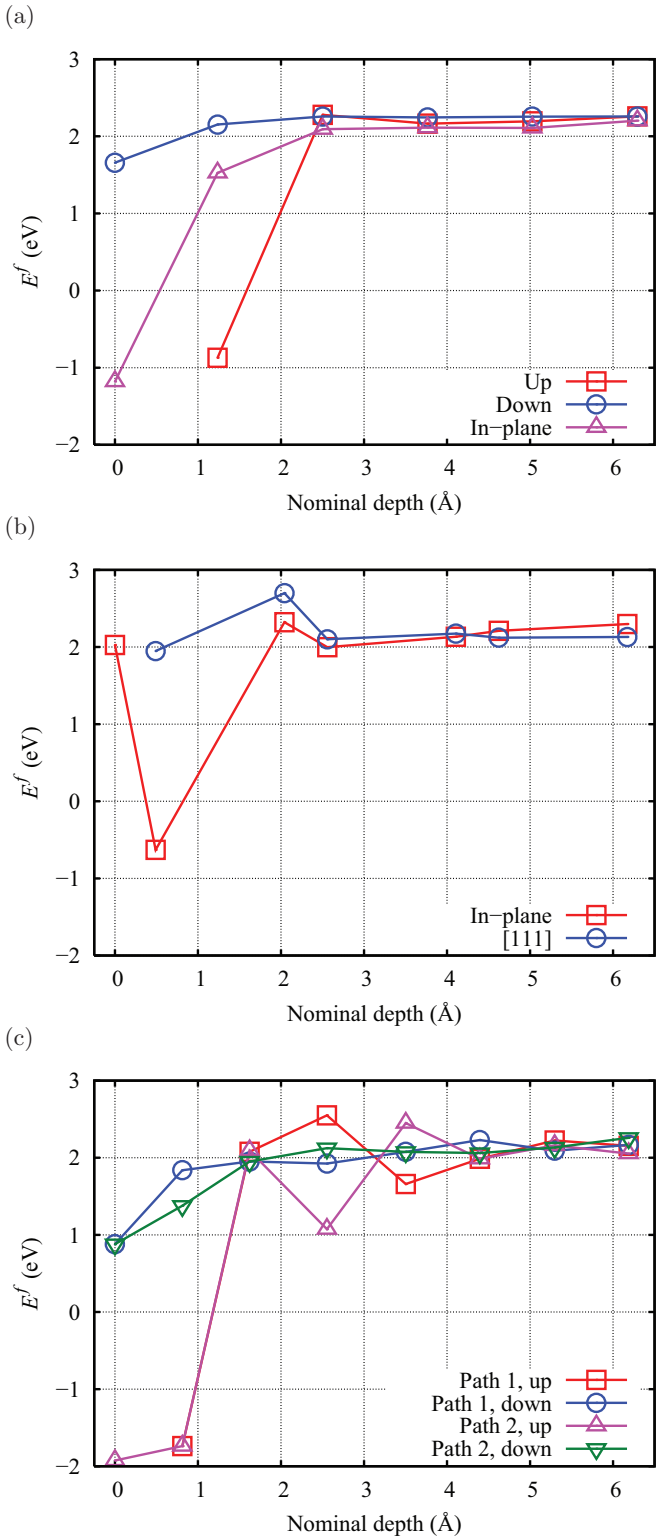

FIG. 6. (Color online) Formation energy of NV in (a) (110), (b) (111), and (c) (001) diamond surfaces as a function depth of the carbon site in pristine diamond (Fig. 1), as specified by Eqs. (2). Symbol and labels follow the definitions in Fig. 2.

is responsible for the three lowest many-body states of the defect when in the negative charge state.[61] However, when close to the surface of the diamond, the lowering of the symmetry results in a raising of this degeneracy,[62] and where the defect is in the uppermost layer, it may well be expected that even the number of dangling bonds will differ. As with N_s, we start with the results for the (110) surface, and the calculated formation energies as a function of depth are plotted in Fig. 6(a).

Variation in formation energy with position is only significant in the uppermost three layers. Where nitrogen is in the uppermost layer and the vacancy is adjacent to it (i.e., also in the uppermost layer), two of the three dangling bonds are eliminated. The structure [Fig. 7(d)] has a calculated formation energy of −1.2 eV. Where nitrogen is in the second layer and the vacancy is in the first, again only one dangling bond remains [Fig. 7(e)] with a correspondingly low formation energy of −0.9 eV. Thus we find that the orientation of NV centers within the (110) growth plane is thermodynamically more favorable than that out of the surface. In other words, based upon NV formation energies, it appears that the preferential orientation of NV centers out of the surface in (110)-grown diamond cannot be explained. However, we shall show in Sec. III D that this is not the case.

The favorable formation energy of the NV centers is only present in the upper two layers in the (110) surface. For NV incorporated deeper within the diamond, it cannot be formed with fewer than three dangling bonds.

NV may exist in the negative charge state, and in Fig. 8 the variation in the acceptor level with location is plotted. Based upon an acceptor level around midgap, all locations of NV within the (110) surface remain acceptors, the electrical level being generated by the presence of at least one carbon radical.

The dramatic formation energy variation seen for the (110) surface is also present in the other two surfaces [Figs. 6(b) and 6(c)]. In the (111) surface with N in the second layer and the vacancy in the first, a single dangling bond is present, leading to a formation energy of −0.6 eV. Similarly, for the (001) surface, sites in the upper layers may result in a single radical, and it is in this surface orientation that the formation energy of the NV center has the lowest value determined out of the three low-index surfaces examined in this study. When N lies in either the first or second layers, and the vacancy lies in the uppermost carbon layer, the formation energies reflect that there is only one radical carbon site, being between −1.9 and −1.5 eV. These structures are 0.3–0.7 eV lower in energy than the most favorable form on the (110) surface, and 0.9–1.2 eV lower in energy than the (111) surface. The differences seen here for the energies as a function of surface orientation are in line with previous studies,[63] where the energies of substitutional impurities were found to exhibit similar variations.

Overall, the formation energies of NV centers in the diamond surfaces are much higher than the corresponding N_s defects. Both forms of nitrogen share substantial stabilization in the uppermost carbon layer due to the removal of dangling bonds, which requires the removal of a hydrogen atom in the case of N_s. The relative energies of N_s and NV shall be revisited in Sec. III D, but first we move the hydrogen-decorated NV centers, NVH.

C. NVH centers

The formation energies as a function of depth for NVH are plotted in Fig. 9. The introduction of hydrogen to the NV

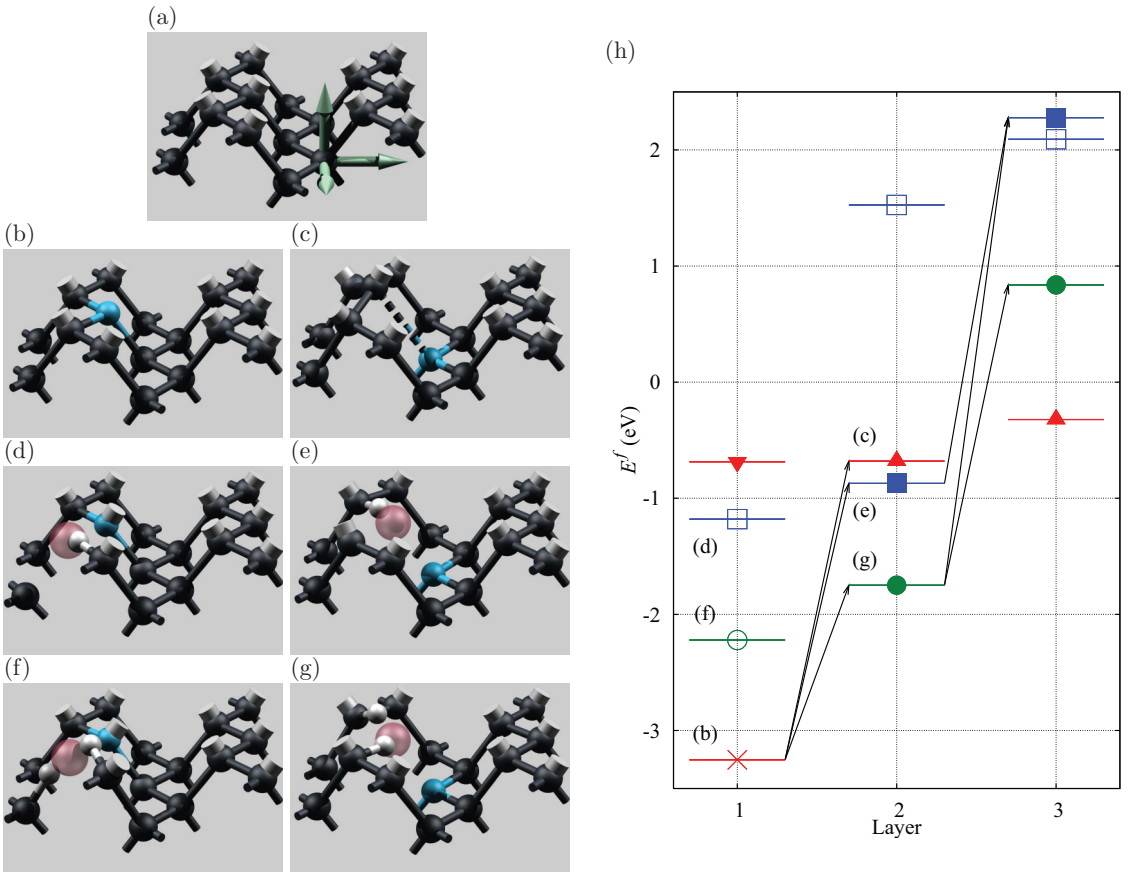

FIG. 7. (Color online) Schematic perspective structures of N_s, NV, and NVH in the (110):H surface. Black, blue, and white spheres represent C, N, and H, respectively, with red, translucent spheres indicating the vacancy. For clarity, surfaces H are not plotted but their direction is indicated by white stumps. Part (a) shows a section of defect-free surface, with arrows indicating the [001] (right) [$\bar{1}$10] (out of the page) and [110] directions. Parts (b), (d), and (f) show N_s, NV, and NVH, where N lies in the uppermost carbon layer, and (c), (e), and (g) show the same centers in the second layer. Part (h) shows a plot of the calculated formation energy for the uppermost three layers. Triangles, circles, and squares indicate N_s, NVH, and NV, respectively, with the cross indicating N_s at the surface with H removed. Filled (empty) symbols indicate polarization of the centers out of (within) a (110) plane. NV and NVH polarized out of a (110) plane have N deeper within the surface than the vacancy, and for N_s the up- and down-pointing symbols show the broken bond pointing out of and into the surface, respectively. Labeling in (h) indicates associated structures depicted, and the arrows indicating possible production paths are explained in the text.

centers lowers the symmetry of the center in bulk diamond, increasing the number of possible orientations. However, it is known that the hydrogen atom can readily reorient between carbon sites, and to simplify the graphical presentation, we include only the energies for the most favorable location of the hydrogen for each orientation of the underlying NV center.

The shapes of the energy profiles resemble those of NV plotted in Fig. 6, but they are offset downward in energy by 0.5–1.0. This reduction is due to the fact that there are fewer radicals in all layers. For the (110) surface, NVH has the lowest energy, with nitrogen in the first layer and the vacancy in the same layer [Fig. 7(f)], having a formation energy of −2.2 eV. Then, with nitrogen in the second layer and the vacancy in the first [Fig. 7(g)], the energy rises to −1.7 eV. As with the case for the undecorated NV center, this suggests that on a simple basis of formation energies, a polarization within the growth plane would be preferred, at odds with the observed polarization. We shall return to this issue in Sec. III D.

There is a relatively small reduction in formation energy with the addition of hydrogen for NVH in the upper layers of the (111), and for the (001) surface NVH is very stable, with the most favorable formation energy of any surface examined in this study. The lowest energy of NVH arrangement places nitrogen in the second layer with the vacancy in the first, with a formation energy of −3.4 eV, but with both components in the first carbon layer, the formation energy is still very low at −3.0 eV.

In terms of the electrical properties, it is known that NVH has an acceptor level when in bulk diamond, but at the surface, where there are no carbon radicals, the acceptor level is moved by around 2 eV toward the conduction band (Fig. 10), a much greater effect than calculated for NV (Fig. 8). Indeed, it is likely that this shift reflects an absence of an acceptor level in the cases in which there are no unsaturated carbon atoms.

D. N_s, NV, and NVH and the origin of polarization

We shall start with the (110) surface, where the incorporation of NV and NVH centers has been shown in experiment to be 100% polarized, involving trigonal axes of the centers along

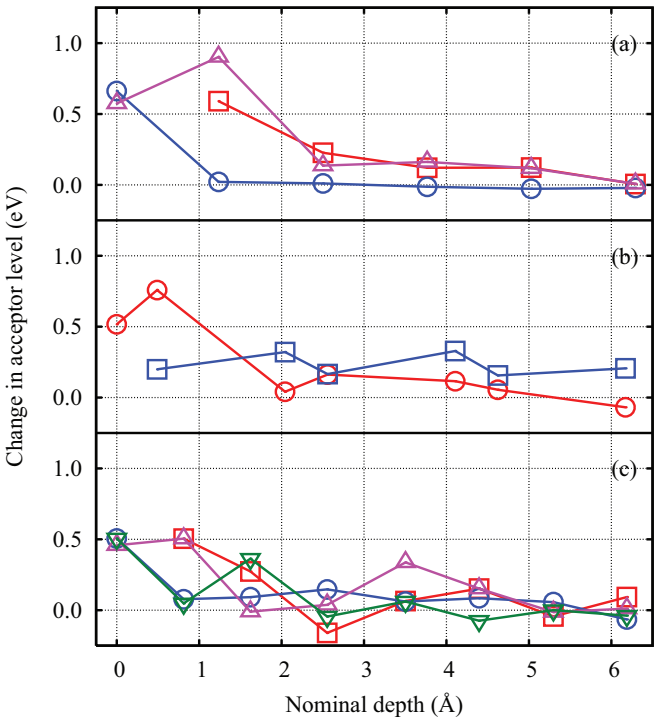

FIG. 8. (Color online) Calculated changes in acceptor level for NV in (a) (110), (b) (111), and (c) (001) diamond surfaces and as a function of depth. A positive change indicates that the level is moving upward in energy, away from the valence-band top. Symbols follow the definition in Fig. 2.

[111] and [11$\bar{1}$], and none along [1$\bar{1}$1] or [$\bar{1}$11]. This means that the vacancies and N atoms lie in different (110) planes. As shown in Secs. III B and III C, the calculated formation energies seem to imply that [111] and [11$\bar{1}$] orientations are energetically less favorable, in apparent contradiction with the observations. However, these energies compare only the orientations preferred under thermodynamic equilibrium, and they take no account of the sequence of events that lead to the incorporation within the lattice.

Since isolated lattice vacancies are mobile at growth temperatures, it seems most probable that in a stepwise formation process the nitrogen atom is incorporated first, and the vacancy second, during the formation of either NV or NVH. Indeed, there is some support in our calculations for such a picture in the energies of the structures where nitrogen is in the uppermost layer of the diamond, and a vacancy lies in the second layer. For both NV and NVH centers in all three surfaces, incorporation of a vacancy before the nitrogen atom results in a much higher energy configuration than the reverse (Figs. 6 and 9). For example, in the (110) surface, nitrogen in the first carbon layer and a vacancy in the second have a calculated formation energy of around +1.7 eV [circle at a nominal depth of zero, Fig. 6(a)], whereas the two components in reverse order have a formation energy of around −0.9 eV [square at a nominal depth of 1.2 Å, Fig. 6(a)], a difference of 2.6 eV.

If we assume that the order of incorporation of the two components is correctly described as nitrogen followed by the vacancy, by far the most stable form for the initial stage of

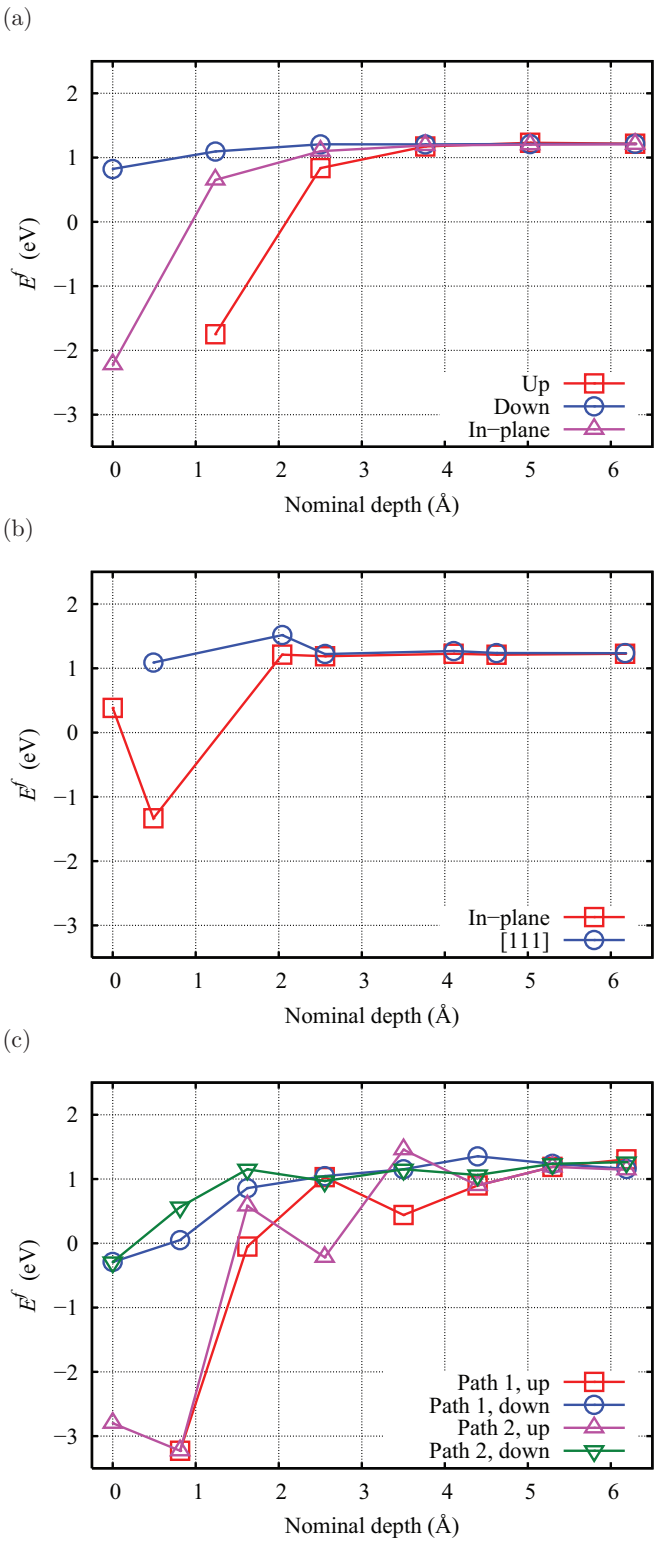

FIG. 9. (Color online) Formation energy of NVH in (a) (110), (b) (111), and (c) (001) diamond surfaces as a function depth of the carbon site in pristine diamond (Fig. 1), as specified by Eq. (2). Symbol and labels follow the definitions in Fig. 2.

incorporation of substitutional nitrogen is N in the surface layer with no hydrogen bonded to it [Fig. 7(b)]. This form of nitrogen is calculated to have an absolute formation energy

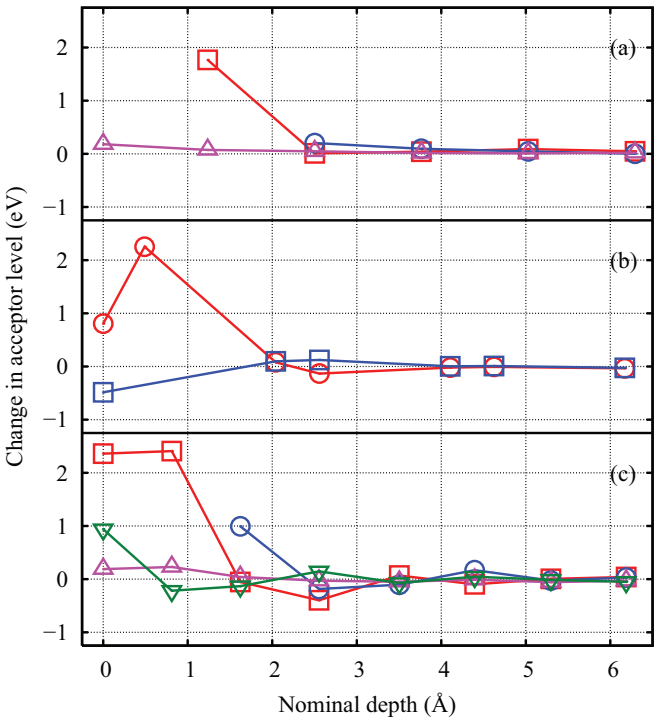

FIG. 10. (Color online) Calculated changes in acceptor level for NVH in (a) (110), (b) (111), and (c) (001) diamond surfaces and as a function depth. A positive change indicates that the level is moving upward in energy, away from the valence-band top. Symbols follow the definition in Fig. 2.

of around −3.2 eV. Such a defect is not only the most stable form for N_s in the (110) surface, it is also much more stable than either NV [Fig. 7(d)] or NVH [Fig. 7(f)], with formation energies of −1.2 and −2.2 eV, respectively. It is perhaps helpful to focus on the number of dangling bonds in each case. N_s in the surface is completely chemically satisfied, NV in the surface has a single dangling bond, and NVH has no unsaturated atoms and is therefore chemically as stable as N_s. A key difference between N_s and NVH in the uppermost layer is the steric repulsion between the H atoms saturating the vacant site. From a statistical thermodynamics perspective, the formation energies suggest that in-plane polarized NV and NVH centers are very improbable relative to N_s.

We next suppose that another atomic layer of carbon is deposited on the (110) surface, covering the layer containing the N atom. In terms of the calculated properties presented in Secs. III A–III C, the additional layer of carbon means we need to consider the energetics of N in the second layer. In contrast to the case with N in the surface, where N is buried by a layer of carbon, N_s is much less energetically favored. We have considered both a simple substitution of carbon by N, resulting in a P1-like center [Fig. 7(c)], and a structure where a nearby hydrogen atom has been removed from a carbon atom at the surface, resulting is an on-site, ionized nitrogen donor center, and a surface carbon site which traps the donated electron. It turns out in our calculations that both of these structures result in a formation energy of around −0.7 eV, some 2.5 eV higher than that of N on the surface [Fig. 7(b)].

We now suppose the addition of a vacancy. If it is to be associated with the nitrogen lying in the second layer, then it is then expected to grow into the first layer, since a vacancy preexisting in the diamond surface is unlikely based upon its relatively high formation energy[64] and mobility at the growth temperature. The NV or NVH resulting from the addition of a vacancy to a nitrogen atom in the second layer will be polarized "out of the surface." We find such a structure to have favorable formation energies in comparison to a N_s center buried in the second layer, being around −0.9 and −1.7 eV, respectively (Figs. 6 and 9). This is a crucial result: it means that NV is comparable in energy to N_s in the second layer, with that of NVH considerably more favorable.

Finally, it is supposed that subsequent layers will bury the NV or NVH centers, leading to the polarization, provided that the centers are unable to reorient, which is expected to be the case based upon the calculated reorientation barriers[65] and temperatures at which the centers are found to be stable in experiment.[40,47]

Indeed, although reorientation of NV in bulk diamond is thought[65] to involve processes with a barrier greater than 5 eV, we cannot entirely exclude the possibility that there are lower-energy routes between the two polarizations of, say, NV when very close to the surface layers. We have therefore calculated the barrier to reorientation between NV shown in Fig. 7(e) and a form where the vacancy lies in the second carbon layer, adjacent to N. The forward and reverse reactions are calculated to be activated by energies of 5.0 and 4.4 eV, respectively. Based upon these energies, and their consistency with the bulk reorientation/diffusion energies, we conclude that it is unlikely that any reorientation of this type would take place at growth temperatures.

Combining these data, we therefore have a quantitative energy description for the route to formation of both NV and NVH in the (110) surface that explains the geometric polarization. Indeed, it is a natural consequence of these incorporation stages that both vacancy-containing defects *should* be present in diamond. This will happen despite their bulk formation energies being 1 and 2 eV higher in energy than N_s, which on a simple thermodynamic basis would suggest that they should not be formed.

The energetics at each stage are summarized in Fig. 7(h), with the arrows indicating the possible steps that could take place by incremental addition of layers of carbon such that nitrogen is incorporated first, and a vacancy potentially incorporated second. The arrows exclude any sequence that would require reorientation of a vacancy-containing center, and in this case the most favorable sequences on an energy basis can only result in polarization as seen in experiment.

Turning to (111) surfaces, a mechanism for incorporation of NV or NVH is much less clear. As with the (110) surface, initial incorporation of nitrogen seems likely to be a nitrogen substituting for a C–H group at the surface. (111) diamond growth is thought to proceed by bilayer addition, rather than the monolayer process on the (110) surface, so if nitrogen is incorporated as we suggest, one might then expect nitrogen only to appear on the odd-numbered layers in the simulations performed for this study. All NV and NVH centers with the nitrogen in odd layers (first, third, fifth, etc.) have formation energies which are much higher than N_s, so any polarization in the (111) growth surfaces must proceed by another mechanism.

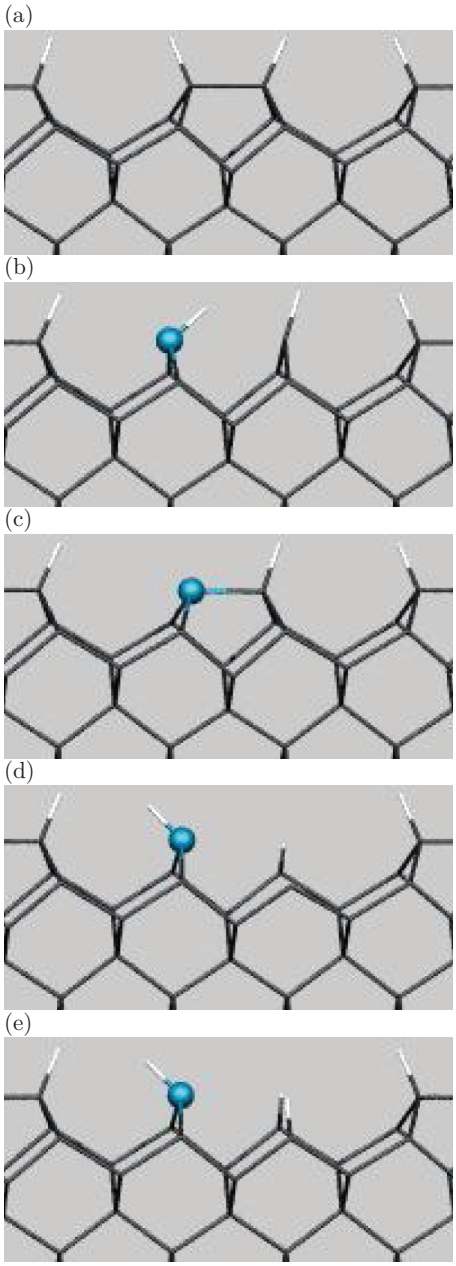

FIG. 11. (Color online) Schematics of the structures of most stable forms of (b) and (c) N_s, (d) NV, and (e) NVH in the (001) surface. Part (a) is the corresponding defect-free section, for comparison. Colors are as in Fig. 1. [001] is vertically up, with the projection and horizontal direction being [1$\bar{1}$0] and [110], respectively.

Finally, we turn to the (001) surface. Here, there is no route to polarization as the surface normal direction has an equal projection onto all defect orientation directions. However, as with the (110) surface, the energetics provides a route to formation of the vacancy-containing centers. Initially, as with both the (110) and (111) surface orientations, the substitution of a surface C–H group by a nitrogen atom is highly energetically favorable, with a formation energy of −3.0 eV. In contrast to the other surfaces, formation of NVH centers in the uppermost carbon layer is comparable to N_s, with a formation energy of −2.8 eV. However, this comparison has to be viewed with some caution. Figures 11(b)–11(e) show the structures of most stable forms of N_s, NV, and NVH in the (001) surface. The low-energy form of NVH can be viewed as a component of a step in the (001) surface, and might be less susceptible to encapsulation than the corresponding defects in more densely packed surfaces. Nevertheless, the formation of both NV and NVH, where the N atom lies in the second layer, is much lower in energy than the formation of N_s, and following a similar argument to that proposed for the (110) surface, this provides a mechanism for the growing in of these relatively high-energy defects.

IV. CONCLUSIONS

N_s, NV, and NVH centers in the first few layers of (110), (111), and (001) surfaces have been modeled to investigate their energetics. The results for the (110) surface have provided a clear guide to the mechanism of incorporation of the vacancy-containing centers, and the reason for their orientational polarization. We confirm that the sequence proposed[45] for the inclusion of the vacancy-containing defects correspond to an energetically favorable route, with nitrogen substituting at the surface first, and then association of a lattice vacancy and possibly a hydrogen atom with the N atom when the next atomic layer is deposited.

A second important consequence of the relative energies of the three defects lies in the fact that the vacancy-containing defects are incorporated in the diamond at all. Noting that the formation energies of the NV and NVH centers exceed that of N_s by around 2.2 and 1.2 eV, respectively, the statistical thermodynamic ratio of N_s to a vacancy-containing center may be obtained roughly from the factor $\exp(-\Delta E/k_B T)$, where ΔE is the energy difference noted here, k_B is Boltzmann's constant, and T is the absolute temperature. This factor would suggest that $[N_s]/[NV]$ and $[N_s]/[NVH]$ would be of the order of 10^7 and 10^4, respectively, at 1400 °C. This admittedly crude estimate would suggest that in practice the NV and NVH centers should not be easily observed in as-grown CVD diamond. However, because the formation energies of NV and NVH centers are so much lower when in the upper two or so layers of the growing diamond, they can be incorporated, and then become fixed in the diamond in supersaturation due to the very high barriers to migration.

These results specific to the incorporation of nitrogen-containing defects are likely to have relevance to the incorporation of other impurities, with boron, silicon, and phosphorus being particularly significant cases. We expect that the general principle of the stabilization of vacancy-impurity complexes in the uppermost layers of a growing diamond is also the case for these species. The evidence of the incorporation of silicon-vacancy complexes may therefore have a similar explanation to that of NV and NVH, but the B and P cases are much less obvious as there is meager evidence for the formation of B-V or P-V complexes. These impurities will be the subject matter of a future study.

Finally, we also note that the mechanism of NV and NVH incorporation leading to orientational polarization also provides some insight into the way in which the diamond itself is growing, and further studies to illuminate these relations will be of great importance.

ACKNOWLEDGMENTS

This work made use of the facilities of N8 HPC provided and funded by the N8 consortium and EPSRC (Grant No. EP/K000225/1). The Centre is coordinated by the Universities of Leeds and Manchester.

*mohammed.atumi@ncl.ac.uk

[1]H. Windischmann, in *Properties, Growth and Applications of Diamond*, No. 26 in *EMIS Datareviews Series*, edited by M. H. Nazaré and A. J. Neves (INSPEC, Institute of Electrical Engineers, London, 2001), Chap. C2.2, pp. 410–415.

[2]J. E. Butler, M. W. Geis, K. E. Krohn, J. Lawless, Jr., S. Deneault, T. M. Lyszczarz, D. Flechtner, and R. Wright, Semicond. Sci. Technol. **18**, S67 (2003).

[3]J. Isberg, J. Hammersberg, E. Johansson, T. Wikström, D. J. Twitchen, A. J. Whitehead, S. E. Coe, and G. A. Scarsbrook, Science **297**, 1670 (2002).

[4]K. Thonke, Semicond. Sci. Technol. **18**, S20 (2003).

[5]C. Johnston, A. Crossley, M. Werner, and P. R. Chalker, in *Properties, Growth and Applications of Diamond*, No. 26 in *EMIS Datareviews Series*, edited by M. H. Nazaré and A. J. Neves (INSPEC, Institute of Electrical Engineers, London, 2001), Chap. B3.3, pp. 337–347.

[6]J. Kačmarčik, C. Marcenat, C. Cytermann, A. Ferreira de Silva, L. Ortega, F. Gustafsson, J. Marcus, T. Klein, E. Gheeraert, and E. Bustarret, Phys. Status Solidi A **202**, 2160 (2005).

[7]E. Bustarret, J. Kačmarcik, C. Marcenat, E. Gheeraert, C. Cytermann, J. Marcus, and T. Klein, Phys. Rev. Lett. **93**, 237005 (2004).

[8]A. Badzian and T. Badzian, Appl. Phys. Lett. **62**, 3432 (1993).

[9]M. E. Zvanut, W. E. Carlos, J. A. Freitas, Jr., K. D. Jamison, and R. P. Hellmer, Appl. Phys. Lett. **65**, 2287 (1994).

[10]S. Jin and T. D. Moustakas, Appl. Phys. Lett. **65**, 403 (1994).

[11]R. Farrer, Solid State Commun. **7**, 685 (1969).

[12]S. A. Kajihara, A. Antonelli, J. Bernholc, and R. Car, Phys. Rev. Lett. **66**, 2010 (1991).

[13]P. R. Briddon, R. Jones, and M. I. Heggie, in *Proceedings of the International Conference on New Diamond Science and Technology*, edited by R. Messier, J. T. Glass, J. E. Butler, and R. Roy (Materials Research Society, Pittsburgh, 1991), p. 63.

[14]P. R. Briddon and R. Jones, Physica B **185**, 179 (1993).

[15]R. Jones and J. P. Goss, in *Properties, Growth and Applications of Diamond*, No. 26 in *EMIS Datareviews Series*, edited by M. H. Nazaré and A. J. Neves (INSPEC, Institute of Electrical Engineers, London, 2001), Chap. A5.1, pp. 127–129.

[16]E. B. Lombardi, A. Mainwood, and K. Osuch, Diamond Relat. Mater. **12**, 490 (2003).

[17]K. M. Etmimi, M. E. Ahmed, P. R. Briddon, J. P. Goss, and A. M. Gsiea, Phys. Rev. B **79**, 205207 (2009).

[18]R. Jones, J. P. Goss, and P. R. Briddon, Phys. Rev. B **80**, 033205 (2009).

[19]R. Ulbricht, S. T. van der Post, J. P. Goss, P. R. Briddon, R. Jones, R. U. A. Khan, and M. Bonn, Phys. Rev. B **84**, 165202 (2011).

[20]L. du Preez, Ph.D. thesis, University of the Witwatersrand, Johannesburg, 1965.

[21]G. Davies and M. F. Hamer, Proc. R. Soc. London, Ser. A **348**, 285 (1976).

[22]J. P. Goss, P. R. Briddon, M. J. Rayson, S. J. Sque, and R. Jones, Phys. Rev. B **72**, 035214 (2005).

[23]Y. Mita, Phys. Rev. B **53**, 11360 (1996).

[24]X.-F. He, N. B. Manson, and P. T. H. Fisk, Phys. Rev. B **47**, 8816 (1993).

[25]J. P. Goss, P. R. Briddon, S. J. Sque, and R. Jones, Diamond Relat. Mater. **13**, 684 (2004).

[26]J. R. Weber, W. F. Koehl, J. B. Varley, A. Janotti, B. B. Buckley, C. G. van de Walle, and D. D. Awschalom, Proc. Natl. Acad. Sci. (USA)) **107**, 8513 (2010).

[27]N. Mizuochi, T. Makino, H. Kato, D. Takeuchi, M. Ogura, H. Okushi, M. Nothaft, P. Neumann, A. Gali, F. Jelezko, J. Wrachtrup, and S. Yamasaki, Nat. Photon. **6**, 299 (2012).

[28]J. W. Steeds, S. J. Charles, J. Davies, and I. Griffin, Diamond Relat. Mater. **9**, 397 (2000).

[29]J. Wrachtrup and F. Jelezko, J. Phys. Condens. Matter **18**, S807 (2006).

[30]F. Jelezko, T. Gaebel, I. Popa, M. Domhan, A. Gruber, and J. Wrachtrup, Phys. Rev. Lett. **93**, 130501 (2004).

[31]G. Balasubramanian1, I. Y. Chan, R. Kolesov, M. Al-Hmoud, J. Tisler, C. Shin, C. Kim, A. Wojcik, P. R. Hemmer, A. Krueger, T. Hanke, A. Leitenstorfer, R. Bratschitsch, F. Jelezko, and J. Wrachtrup, Nature (London) **455**, 648 (2008).

[32]C. L. Degen, Appl. Phys. Lett. **92**, 243111 (2008).

[33]J. R. Maze, P. L. Stanwix, J. S. Hodges, S. Hong, J. M. Taylor, P. Cappellaro, L. Jiang, M. V. G. Dutt, E. Togan, A. S. Zibrov, A. Yacoby, R. L. Walsworth, and M. D. Lukin, Nature (London) **455**, 644 (2008).

[34]S. Steinert, F. Dolde, P. Neumann, A. Aird, B. Naydenov, G. Balasubramanian, F. Jelezko, and J. Wrachtrup, Rev. Sci. Instrum. **81**, 043705 (2010).

[35]G. Balasubramanian, P. Neumann, D. Twitchen, M. Markham, R. Kolesov, N. Mizuochi, J. Isoya, J. Achard, J. Beck, J. Tissler, V. Jacques, P. R. Hemmer, F. Jelezko, and J. Wrachtrup, Nat. Mater. **8**, 383 (2009).

[36]J. M. Taylor, P. Cappellaro, L. Childress, L. Jiang, D. Budker, P. R. Hemmer, A. Yacoby, R. Walsworth, and M. D. Lukin, Nat. Phys. **4**, 810 (2008).

[37]F. Dolde, H. Fedder, M. W. Doherty, T. Nöbauer, F. Rempp, G. Balasubramanian, T. Wolf, F. Reinhard, L. C. L. Hollenberg, F. Jelezko, and J. Wrachtrup, Nat. Phys. **7**, 459 (2011).

[38]C. Glover, M. E. Newton, P. Martineau, D. J. Twitchen, and J. M. Baker, Phys. Rev. Lett. **90**, 185507 (2003).

[39]J. P. Goss, P. R. Briddon, R. Jones, and S. Sque, J. Phys. Condens. Matter **15**, S2903 (2003).

[40]R. U. A. Khan, P. M. Martineau, B. L. Cann, M. E. Newton, and D. J. Twitchen, J. Phys. Condens. Matter **21**, 364214 (2009).

[41]J. P. Goss, P. R. Briddon, H. Pinho, and R. Jones, Phys. Status Solidi A **207**, 2049 (2010).

[42]H. Pinto, R. Jones, J. P. Goss, and P. R. Briddon, J. Phys. Conf. Ser. **281**, 012023 (2011).

[43] A. Kerridge, A. H. Harker, and A. M. Stoneham, J. Phys. Condens. Matter **16**, 8743 (2004).
[44] M. J. Shaw, P. R. Briddon, J. P. Goss, M. J. Rayson, A. Kerridge, A. H. Harker, and A. M. Stoneham, Phys. Rev. Lett. **95**, 105502 (2005).
[45] A. M. Edmonds, U. F. S. D'Haenens-Johansson, R. J. Cruddace, M. E. Newton, K. M. C. Fu, C. Santori, R. G. Beausoleil, D. J. Twitchen, and M. L. Markham, Phys. Rev. B **86**, 035201 (2012).
[46] T. Evans and Z. Qi, Proc. R. Soc. London, Ser. A **381**, 159 (1982).
[47] A. T. Collins, J. Phys. C **13**, 2641 (1980).
[48] J. P. Perdew, K. Burke, and M. Ernzerhof, Phys. Rev. Lett. **77**, 3865 (1996).
[49] M. J. Rayson and P. R. Briddon, Comput. Phys. Commun. **178**, 128 (2008).
[50] P. R. Briddon and R. Jones, Phys. Status Solidi B **217**, 131 (2000).
[51] J. P. Goss, M. J. Shaw, and P. R. Briddon, in *Theory of Defects in Semiconductors*, Vol. 104 of *Topics in Applied Physics*, edited by D. A. Drabold and S. K. Estreicher (Springer, Berlin, 2007), pp. 69–94.
[52] M. J. Rayson and P. R. Briddon, Phys. Rev. B **80**, 205104 (2009).
[53] S. J. Sque, R. Jones, and P. R. Briddon, Phys. Rev. B **73**, 085313 (2006).
[54] A. K. Tiwari, J. P. Goss, P. R. Briddon, N. G. Wright, A. B. Horsfall, R. Jones, H. Pinto, and M. J. Rayson, Phys. Rev. B **84**, 245305 (2011).
[55] A. K. Tiwari, J. P. Goss, P. R. Briddon, N. G. Wright, A. B. Horsfall, and M. J. Rayson, Phys. Status Solidi A **209**, 1703 (2012).
[56] J. P. Goss, P. R. Briddon, R. Jones, Z. Teukam, D. Ballutaud, F. Jomard, J. Chevallier, M. Bernard, and A. Deneuville, Phys. Rev. B **68**, 235209 (2003).
[57] H. J. Monkhorst and J. D. Pack, Phys. Rev. B **13**, 5188 (1976).
[58] G. Henkelman, B. P. Uberuaga, and H. Jónsson, J. Chem. Phys. **113**, 9901 (2000).
[59] G. Henkelman and H. Jónsson, J. Chem. Phys. **113**, 9978 (2000).
[60] S. Lany and A. Zunger, Phys. Rev. B **78**, 235104 (2008).
[61] J. P. Goss, R. Jones, S. J. Breuer, P. R. Briddon, and S. Öberg, Phys. Rev. Lett. **77**, 3041 (1996).
[62] H. Pinto, R. Jones, D. W. Palmer, J. P. Goss, P. R. Briddon, and S. Öberg, Phys. Status Solidi A **208**, 2045 (2011).
[63] K. Larsson, Comp. Mater. Sci. **27**, 23 (2003).
[64] R. Q. Hood, P. R. C. Kent, R. J. Needs, and P. R. Briddon, Phys. Rev. Lett. **91**, 076403 (2003).
[65] H. Pinto, R. Jones, D. W. Palmer, J. P. Goss, P. R. Briddon, and S. Öberg, Phys. Status Solidi A **209**, 1765 (2012).